Journal of Energy

VOLUME 75 Number 3 | 2026

journal homepage: http://journalofenergy.com/

The Abilities of TDSF and FDSF in Analysing Voltage Distribution in Different Types of Disc Windings of Power Transformers

Martin Meuser, Ebrahim Rahimpour, Morteza Eslamian

Summary **—Power transformers are required to be engineered to withstand overvoltages encountered throughout their operational lifespan. Typically, transformers are specified and assessed according to standard impulse waveshapes, such as the lightning impulse (1.2/50 µs), chopped lightning impulse, and switching impulse (250/2500 µs). Nonetheless, actual overvoltages within the power system may deviate from these standard test impulses. Consequently, it is essential to assess the severity of measured overvoltage waveshapes from the power system and their potential impact on transformer insulation. In the literature three established approaches for waveshape comparison exist: frequency domain severity factor (FDSF), time domain severity factor (TDSF), and the technique outlined in IEC 60071-2: 2023, Annex I. This study examines the effect of non-standard overvoltages on transformer insulation by employing two severity assessment methodologies: the Frequency Domain Severity Factor (FDSF) and the Time Domain Severity Factor (TDSF). Nonstandard waveshapes are generated through systematic variation of parameters - such as front time, tail time, chopping time, fall time and undershoot - based on those defined in IEC 600763: 2018. This controlled methodology facilitates the isolation of individual waveform parameter influences on internal transient responses. The study applies these waveforms to detailed whitebox single turn models of multiple transformer windings with disc ordinary, partially interleaved, fully interleaved and disc shielded arrangements. With the voltage distribution within the windings the severity of the generated non-standard waveforms is assessed in relation to the standard impulses. Consequently, the validity of the standard-defined waveforms for testing transformer winding insulation is evaluated. The results show that FDSF effectively highlights changes in spectral excitation introduced by fast fronts, short fall times, and large undershoots, whereas TDSF more directly captures localized dielectric stress along critical insulation paths within the winding. The study demonstrates that relying on a single severity metric can be misleading and that a combined FDSF and TDSF assessment provides a more robust basis for judging the insulation relevance of non-standard overvoltage waveforms.**

Keywords **— Transformers, lightning impulse, frequency domain severity factor, time domain severity factor, single turn modelI.-**

I. Introduction

Power transformers are engineered to endure overvoltages that may arise during their operational lifespan. Typically, transformers are specified and tested to withstand standard impulse waveshapes, including lightning impulse (1.2/50 μs), chopped lightning impulse, and switching impulse (250/2500 μs) [1], [2] . Nevertheless, the overvoltages encountered in actual power systems often diverge from these test impulses. Real-world transients, particularly those resulting from switching actions, resonance effects, or lightning events accompanied by reflections, can present non-standard waveshapes. This disparity creates uncertainty in transformer insulation design. Consequently, it is imperative to evaluate the severity of non-standard overvoltage waveshapes within the power system and their impact on transformer insulation. The authors of [3] examine three established methods for comparing measured waveshapes: Frequency Domain Severity Factor (FDSF), Time Domain Severity Factor (TDSF), and the technique outlined in IEC 60071-2: 2023, Annex I [4]. Severity factors offer quantitative metrics to assess the influence of arbitrary waveforms relative to standard reference impulses. These metrics play a critical role in insulation coordination and enable transformer modelling to extend beyond conventional testing parameters. In [5] the authors have already analysed four different non-standard overvoltages by implementing FDSF and TDSF factors along the ordinary disc and layer windings of power transformers. In the current work this approach is extended to different non-standard waveforms and other types of windings.

II. Non-Standard Waveforms

In [6] and [7] the authors studied non-standard overvoltage waveforms that were measured at the 110 kV and 220 kV terminals of a power transformer in a substation. However, in this paper the non-standard waveforms are not extracted from measured field data but rather generated by systematically varying the front and tail times of a standard BIL impulse. This allows the isolation and investigation of the effect of individual waveform parameters on internal transient responses. In this

(Corresponding author: Martin Meuser)

Martin Meuser and Ebrahim Rahimpour are with Technical University of Applied Sciences Würzburg-Schweinfurt, Schweinfurt, Germany (email: martin.meuser@thws.de, ebrahim.rahimpour@thws.de)

Morteza Eslamian is with Hitachi Energy, Bad Honnef, Germany (email: morteza.eslamian@hitachienergy.com)

Martin Meuser, Ebrahim Rahimpour, Morteza Eslamian, The Abilities of TDSF and FDSF in Analysing Voltage Distribution in Different Types of Disc Windings of Power Transformers, Journal of Energy, vol. 75 Number 3 (2026), 61–68
https://doi.org/10.37798/2026753781

© 2026 Copyright for this paper by authors. Use permitted under Creative Commons Attribution-NonCommercial (CC BY-NC) 4.0 International License

TABLE I

PARAMETERS OF NON-STANDARD BIL WAVEFORM

Test Case	Rise Time [μs]	Fall Time [μs]
Reference BIL	1.2	50
Test Case NS1	**0.2**	50
Test Case NS2	**0.6**	50
Test Case NS3	**2.0**	50
Test Case NS4	**3.0**	50
Test Case NS5	**4.0**	50
Test Case NS6	1.2	**20**
Test Case NS7	1.2	**35**
Test Case NS8	1.2	**100**
Test Case NS9	1.2	**150**

TABLE II

PARAMETERS OF NON-STANDARD CHOPPED IMPULSE WAVEFORM

Test Case	Time to Chop [μs]	Undershoot [%]	Fall Time [μs]
Reference LIC	3.7	30	0.3
Test Case NS10	**2.0**	30	0.3
Test Case NS11	**3.0**	30	0.3
Test Case NS12	**4.0**	30	0.3
Test Case NS13	**5.0**	30	0.3
Test Case NS14	3.7	**15**	0.3
Test Case NS15	3.7	**50**	0.3
Test Case NS16	3.7	30	**0.1**
Test Case NS17	3.7	30	**1.0**

study, BIL-waveforms with altered rise times (from 0.2 to 4.0 µs) and tail times (from 20 to 150 µs) are applied to the transformer white-box models representing different types of disc windings. Additionally, the parameters the chopped lightning impulse waveform like time to chop, fall time and undershoot are varied. The shape of the non-standard waveforms that are used in this paper are described in TABLE I and TABLE II. Additionally, they are visually represented in Figure 1 together with a standard BIL impulse waveform and a standard chopped impulse waveform as reference. Even though the amplitude is different for the various windings and impulse types, the fundamental shapes of the non-standard waveforms are always derived with the values from TABLE I and TABLE II.

Additionally, a switching impulse with the rise- and falltime of 250/2500 µs is applied to the tested windings. It is not shown in Figure 1 due to its long duration. It is however used in the calculations of the severity factors as it greatly affects the energy spectral density at low frequencies.

III. SEVERITY FACTORS

In the past different approaches to determine the severity of non-standard waveforms have been developed. The Frequency Domain Severity Factor and the Time Domain Severity Factor are to be named as the most relevant procedures, and they will be introduced and applied in the following chapters. Additionally, IEC 60071-2: 2023, Annex I [4] introduces a methodology to separate given waveforms into different elements and then evaluate them separately. However, this methodology will not be used further in this study.

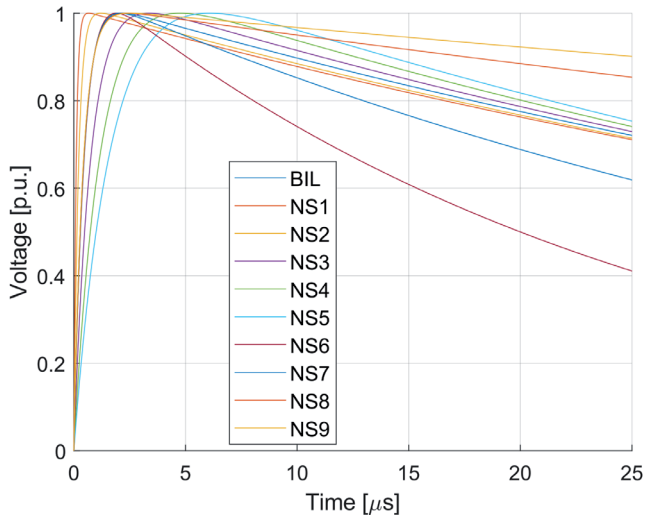

(a) BIL waveforms

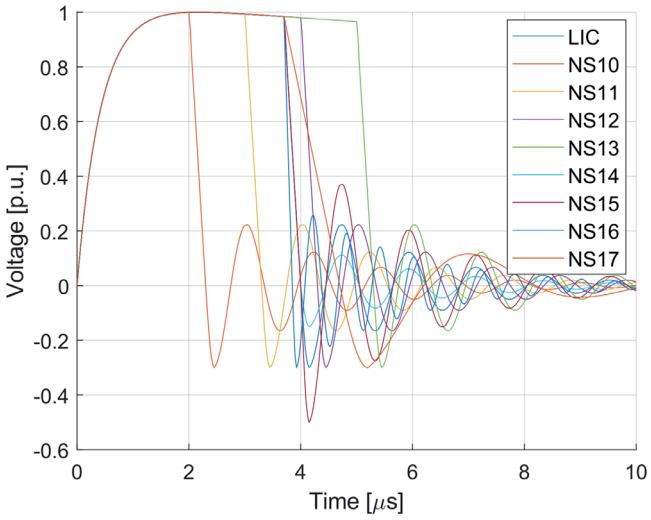

(b) LIC waveforms

Fig. 1. Reference Curves and Non-Standard Waveforms – BIL and chopped wave (LIC)

A. FREQUENCY DOMAIN SEVERITY FACTOR (FDSF)

The FDSF evaluates how strongly a waveform excites the frequency dependent impedance of a winding structure. It is calculated by analysing the energy spectral density (ESD) of the voltage waveform and comparing it with that of a standard reference. This ESD is calculated in the frequency domain from the squared Fast Fourier Transform (FFT) of the time domain waveshape signals. The FDSF was introduced in [8] and extended in [9] and [10]. It is wdefined as follows:

$$\mathrm{FDSF}(\omega) = \frac{\mathrm{ESD}_{\text{non-std}}(\omega)}{\mathrm{ESD}_{\text{envelope}}(\omega)} \tag{1}$$

Where ω represents the angular frequency, $\mathrm{ESD}_{\text{non-std}}(\omega)$ denotes the energy spectral density of the input nonstandard transient voltage applied at transformer terminals, and $\mathrm{ESD}_{\text{envelope}}(\omega)$ indicates the energy spectral density envelope for all standard dielectric tests at the terminals. The energy spectral density of a signal deno-

Martin Meuser, Ebrahim Rahimpour, Morteza Eslamian, The Abilities of TDSF and FDSF in Analysing Voltage Distribution in Different Types of Disc Windings of Power Transformers, Journal of Energy, vol. 75 Number 3 (2026), 61–68
https://doi.org/10.37798/2026753781
© 2026 Copyright for this paper by authors. Use permitted under Creative Commons Attribution-NonCommercial (CC BY-NC) 4.0 International License

tes the energy per unit frequency, indicating the relative amount of energy in different frequency components. It describes the distribution of a wave's energy along the frequency spectrum.

B. Time Domain Severity Factor (TDSF)

The Time domain severity factor is another approach to evaluate the severity of a non-standard waveform that is applied to a transformer winding. It is defined as follows [11], [12]:

$$\mathrm{TDSF}(n) = \frac{\Delta V_{\mathrm{max,NS}}(n)}{\Delta V_{\mathrm{envelope}}(n)} \tag{2}$$

Where $\Delta V_{\mathrm{max,NS}}(n)$ represents the maximum voltage drop along the nth dielectric path caused by a non-standard waveform, and $\Delta V_{\mathrm{envelope}}(n)$ denotes the maximum voltage drop along the nth dielectric path during all standard dielectric tests. In the context of power transformers and reactors, these dielectric paths refer to the insulation gaps between adjacent discs or turns within a winding. Here in this paper the focus is on the voltage drop across the first turn and the voltage drop of the first axial oil duct as well as an oil duct in the middle of the windings and the last oil duct.

Figure 2 presents an algorithm to calculate the TDSF as described in [12]. The initial step of the TDSF approach involves calculating the transient voltage waveform using a power system model along with the terminal model (blackbox) of the transformer. The transient waveform is then applied to a detailed model (white-box) to calculate the internal voltage distribution along the elements of the winding. Ultimately, the internal voltage distribution is determined for each of the standard dielectric tests, and the TDSF is computed accordingly. While [12] does not explicitly state that the TDSF can be obtained for artificially created nonstandard overvoltages, it is evident that it can be calculated for all given transient waveforms at the transformer terminals. To utilize the TDSF approach, internal voltage distribution inside transformer windings must be calculated. Therefore, it is essential to use a detailed white-box model of the transformer windings. In this case a single turn model of all windings is used.

The FDSF and TDSF approaches provide complementary insights into the impact of non-standard transient waveforms on transformer windings. The FDSF focuses on the frequency content of the applied voltage, highlighting how specific frequencies are excited compared to standard tests. This makes it particularly useful for assessing the overall spectral similarity and excitation profile of the waveform. Conversely, the TDSF evaluates the magnitude of voltage stresses along individual dielectric paths, offering a more targeted measure of insulation stress within the winding structure. By combining both methods, engineers can achieve a more comprehensive assessment of both global and local effects caused by nonstandard overvoltages.

IV. Full Wave Lightning Impulse

In this chapter the FDSF and TDSF are used to analyse the impact of deviations in the BIL waveform. Six windings are examined in this paper whereof two have an ordinary disc winding, two have an interleaved disc winding and two have a shielded disc winding as shown in TABLE III.

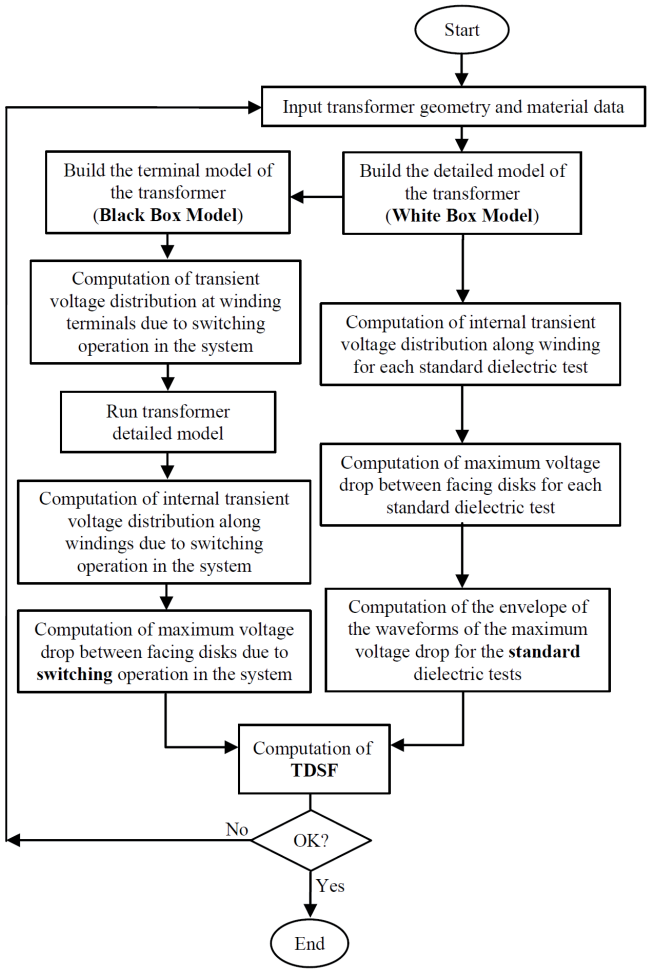

Fig. 2. TDSF algorithm in detail acc. to [12]

Table III

Overview of Tested Windings

Winding Number	Disk type
Winding 1	Ordinary disc
Winding 2	Interleaved disc
Winding 3	Shielded disc
Winding 4	Ordinary disc
Winding 5	Interleaved disc
Winding 6	Shielded disc

The windings under investigation originate from two different transformers, each with a different setup and configurations. The first transformer is rated at 117 MVA and features a voltage ratio of 220 kV to 30 kV. The second transformer has a rated power of 180 MVA and is equipped with windings for three different voltage levels: 230 kV, 115 kV, and 10.5 kV. Notably, the 10.5 kV winding in the second transformer serves as a delta-connected tertiary winding. To facilitate the study of different winding arrangements, the high voltage windings of both transformers were adapted from their original designs. This modification allowed the windings to be configured as ordinary disc, interleaved disc, and shielded disc windings,

Martin Meuser, Ebrahim Rahimpour, Morteza Eslamian, The Abilities of TDSF and FDSF in Analysing Voltage Distribution in Different Types of Disc Windings of Power Transformers, Journal of Energy, vol. 75 Number 3 (2026), 61–68
https://doi.org/10.37798/2026753781
© 2026 Copyright for this paper by authors. Use permitted under Creative Commons Attribution-NonCommercial (CC BY-NC) 4.0 International License

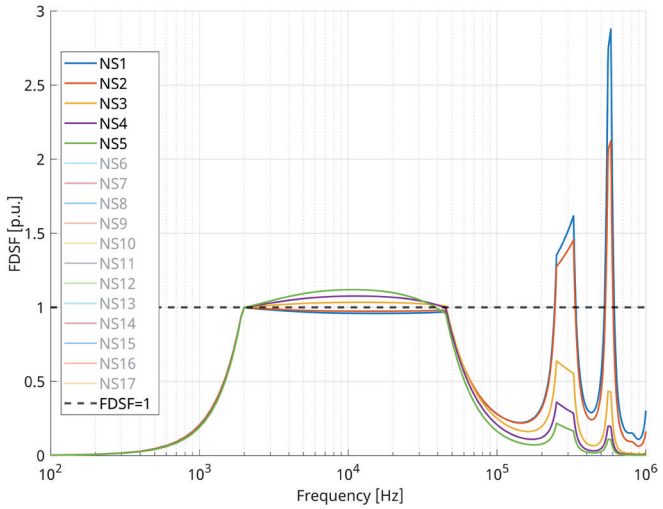

Fig. 3. FDSF of non-standard waveforms with different front times at the input

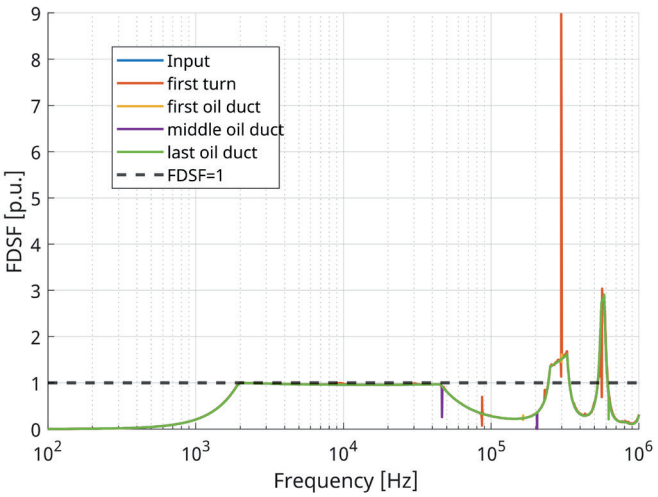

Fig. 4. FDSF at all locations along the winding for non-standard waveform NS1

thereby providing a comprehensive basis for comparative analysis.

All simulation studies were conducted at the nominal tap position. This approach was chosen specifically to minimise the influence of the regulation winding, ensuring that the results reflect the intrinsic properties of the main windings under nominal operating conditions.

A. Front time

The influence of the impulse front time on the Frequency Domain Severity Factor (FDSF) reveals distinct trends across different frequency ranges. Faster front times result in slightly lower FDSF values in the low-frequency range between 2 kHz and 45 kHz, whereas slower front times lead to marginally higher FDSF values within this band. However, faster front times introduce pronounced spectral effects at higher frequencies above 100 kHz. Specifically, two distinct peaks appear in the FDSF spectrum, located between 250 kHz and 327 kHz and between 557 kHz and 580 kHz. In these regions, the FDSF significantly exceeds unity, reaching maximum values of up to 2.9 p.u.

For slower front times, these peaks are still observable but are considerably reduced in magnitude, with FDSF values of approximately 0.5 p.u. This behaviour indicates that fast-rising impulses contain higher-frequency components that more strongly excite the winding's frequency-dependent impedance characteristics.

In addition to evaluating the FDSF at the transformer terminals, the analysis was extended to four internal winding locations: the voltage difference across the first turn, the first axial oil duct, the middle axial oil duct, and the last axial oil duct. To accomplish this the Energy Spectral Density (ESD) of all non-standard curves and reference waveforms is calculated for each winding location individually to compute the FDSF at that location.

For most non-standard waveforms, the FDSF remains nearly identical at all locations along the winding. This unexpected

However, for example winding 5 the FDSF for the shortest front time of 0.2 µs (NS1) shows a significant but very narrow peak of the FDSF at 298 kHz. For NS2 this peak is also present, but lower at about 3 p.u.

In contrast, the Time Domain Severity Factor (TDSF) provides a more differentiated picture. For the shortest front time (NS1), the TDSF at the first turn reaches values close to 2 p.u., indicating a pronounced local stress increase. This value rapidly decreases to approximately 1.35 p.u. at the first oil duct, while the middle and end sections of the winding are only marginally affected. For NS2, the stress at the first turn is reduced to about 1.25 p.u., with a similar decay along the winding. Overall, it can be seen from Figure 5, longer front times consistently result in lower stress levels at the beginning of the winding, while the TDSF approaches unity at the middle and end sections of the windings.

B. Tail time

Varying the tail time of the BIL impulse waveform also has a notable impact on the FDSF spectrum. Longer fall times introduce a distinct peak at approximately 2 kHz, with the peak magnitude increasing as the tail time becomes longer and reaching values close to 2 p.u. for a fall time of 150 µs. Conversely, shorter tail times generate a small peak around 45.3 kHz, where faster decay times lead to higher FDSF values as can be seen in Figure 6.

Unlike the variation in front time, changes in tail time do not significantly affect the FDSF in the higher frequency ranges between 250 kHz and 327 kHz and between 557 kHz and 580 kHz, where the FDSF remains close to unity.

The TDSF analysis in Figure 7 shows that both shorter and longer tail times reduce the stress at the beginning of the winding, including the first turn and the first oil duct. For middle andlonger tail times (NS8 and NS9), however, the stress in the middle and at the end of the winding exceeds unity, indicating a redistribution of voltage stress towards the winding interior.For shorter tail times, the TDSF remains below unity at all investigated locations, suggesting an overall reduction of insulation stress compared to the reference waveform.

Martin Meuser, Ebrahim Rahimpour, Morteza Eslamian, The Abilities of TDSF and FDSF in Analysing Voltage Distribution in Different Types of Disc Windings of Power Transformers, Journal of Energy, vol. 75 Number 3 (2026), 61–68
https://doi.org/10.37798/2026753781
© 2026 Copyright for this paper by authors. Use permitted under Creative Commons Attribution-NonCommercial (CC BY-NC) 4.0 International License

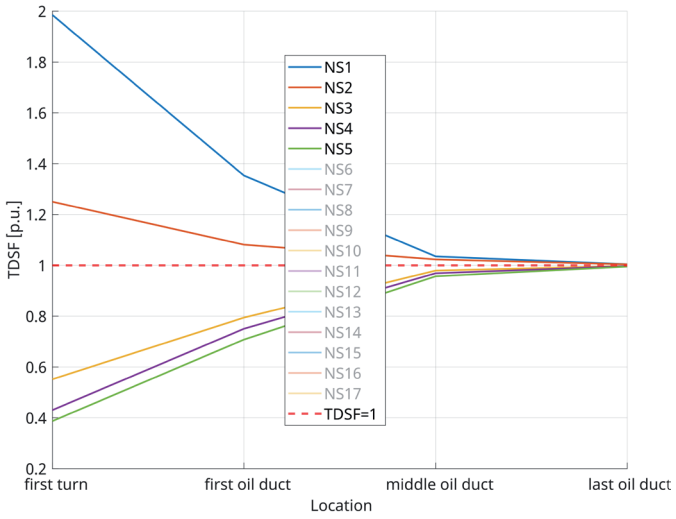

Fig. 5. TDSF at all locations along the winding for non-standard waveforms with different front times (Winding 5)

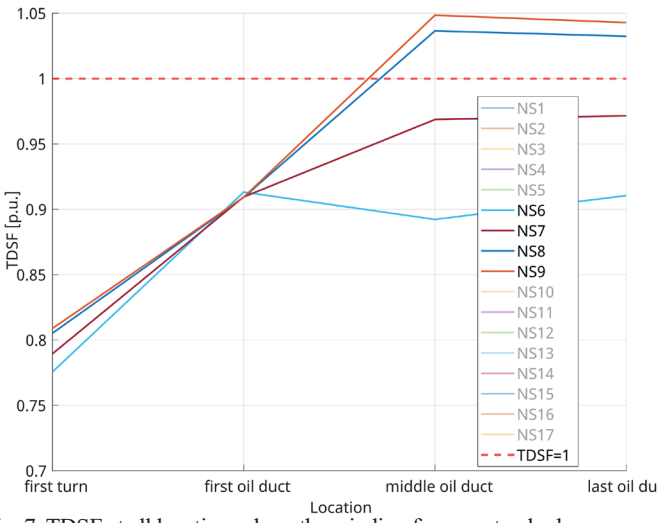

Fig. 7. TDSF at all locations along the winding for non-standard waveforms with different tail times (Winding 5)

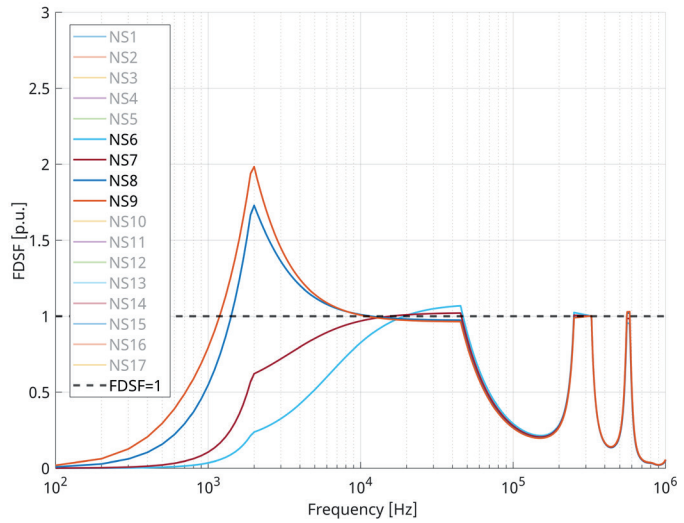

Fig. 6. FDSF of non-standard waveforms with different tail times at the input

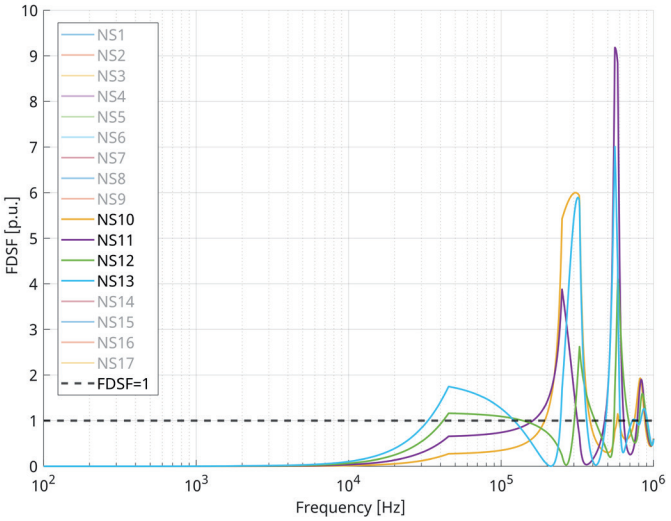

Fig. 8. FDSF of non-standard waveforms with different chopping times at the input

V. Chopped Wave Lightning Impulse

This chapter uses FDSF and TDSF to assess how variations to the chopped wave lightning impulse waveform affect the stress inside the six tested transformer windings.

A. Chopping time

The chopping time is changed from 3.7 µs to 2, 3, 4 and 5 µs. The chopping time strongly affects the frequency content of the applied impulse. When the chopping time is shorter than the reference value of 3.7 µs, pronounced peaks appear in the FDSF spectrum between 250 kHz and 300 kHz as well as around 831 kHz. In addition, a distinctive peak near 558 kHz is observed for a chopping time of 3 µs. For later chopping times, these high-frequency peaks remain present, but an additional peak emerges at approximately 45 kHz, indicating an increased contribution of lower-frequency components.

The TDSF results in Figure 9 show that both earlier and later chopping times can either increase or decrease the stress at the first turn, depending on the winding configuration. In all investigated cases, the stress at the first oil duct remains close to unity and decreases progressively towards the middle and end of the winding. This general trend is consistent across all tested winding types, although the magnitude of the effect varies. Notably, for the ordinary disc winding number four, a shorter chopping time can lead to an increase in stress at the first turn of up to 15 %.

Martin Meuser, Ebrahim Rahimpour, Morteza Eslamian, The Abilities of TDSF and FDSF in Analysing Voltage Distribution in Different Types of Disc Windings of Power Transformers, Journal of Energy, vol. 75 Number 3 (2026), 61–68
https://doi.org/10.37798/2026753781
© 2026 Copyright for this paper by authors. Use permitted under Creative Commons Attribution-NonCommercial (CC BY-NC) 4.0 International License

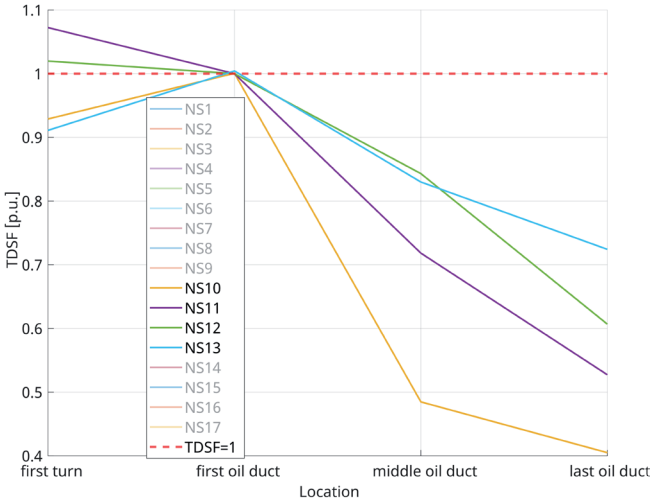

Fig. 9. TDSF at all locations along the winding for non-standard waveforms with different chopping times (Winding 5)

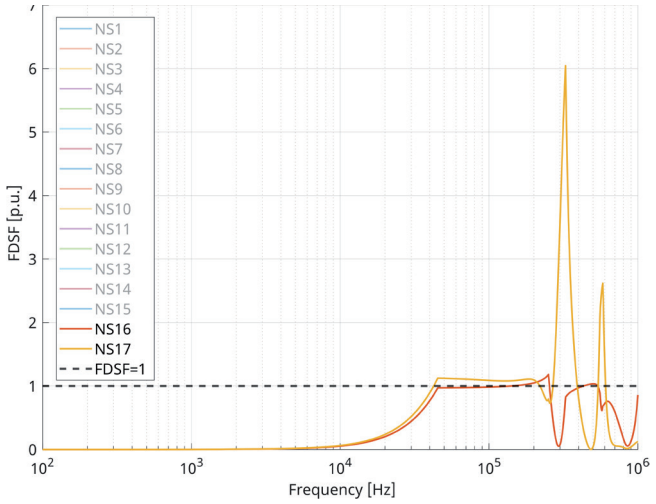

Fig. 10. FDSF of non-standard waveforms with different fall times at the input

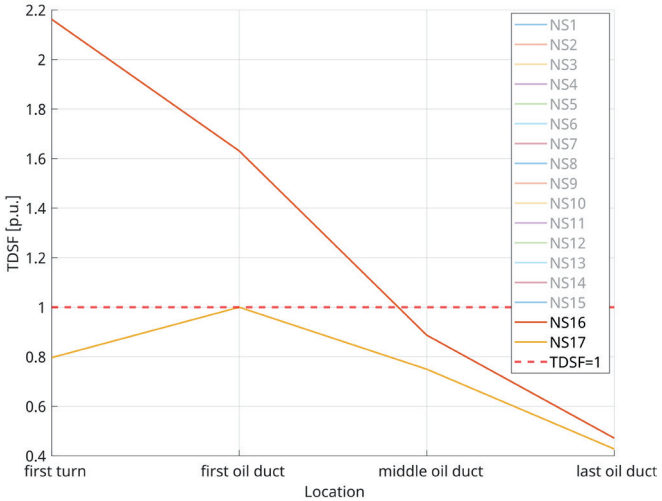

(a) Winding 6

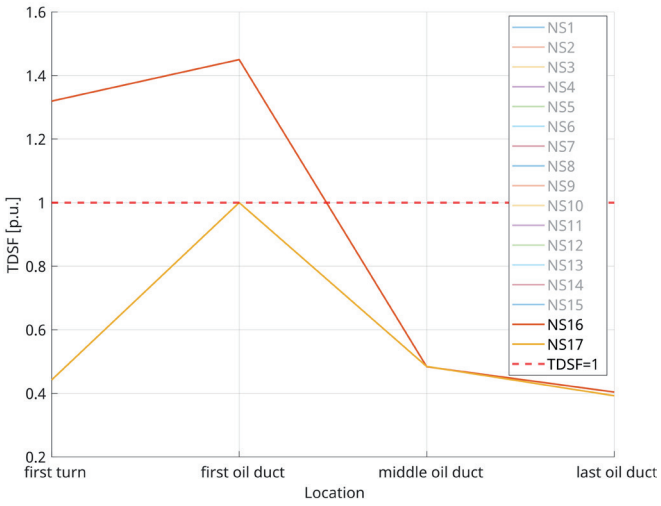

(b) Winding 3

Fig. 11. TDSF at all locations along the winding for non-standard waveforms with different fall times

B. Fall time

The fall time of the chopped impulse primarily influences the high-frequency content of the waveform. Extremely short fall times, such as 0.15 µs, generate frequency components beyond the range of 1 MHz that is analysed here. Within the considered frequency band, a shorter fall time produces two significant FDSF peaks at approximately 326 kHz and 582 kHz, with maximum values reaching up to 6 p.u., as shown in Figure 10. In contrast, a longer fall time of 1 µs does not introduce any pronounced peaks in the FDSF spectrum, indicating a substantially reduced excitation of high-frequency resonances.

The TDSF analysis reveals a consistent behaviour across most windings. Shorter fall times significantly increase the stress at the beginning of the winding, as shown in Figure 11 for the first turn and first oil duct, while the stress at the middle and last oil ducts is reduced to approximately 50 % of the reference value. The TDSF at the first turn varies between 1.7 p.u. and 4 p.u., depending on the winding type. An exception is observed for winding 3, where the maximum TDSF occurs at the first oil duct rather than at the first turn.

C. Undershoot

The undershoot amplitude also affects the severity factors. A lower undershoot level of 15 % does not generate any noticeable peaks in the FDSF spectrum in Figure 12. However, increasing the undershoot to 50 % results in a pronounced FDSF peak of approximately 2.3 p.u. at around 830 kHz. This peak closely corresponds to the oscillatory behaviour following the undershoot in the time-domain waveform.

The TDSF results indicate that higher undershoot amplitudes can significantly increase the stress at the beginning of the winding. Figure 13 shows that for certain winding configurations, such as winding 5, the TDSF at the first oil duct exceeds the value at the first turn. In most cases though,

Martin Meuser, Ebrahim Rahimpour, Morteza Eslamian, The Abilities of TDSF and FDSF in Analysing Voltage Distribution in Different Types of Disc Windings of Power Transformers, Journal of Energy, vol. 75 Number 3 (2026), 61–68
https://doi.org/10.37798/2026753781
© 2026 Copyright for this paper by authors. Use permitted under Creative Commons Attribution-NonCommercial (CC BY-NC) 4.0 International License

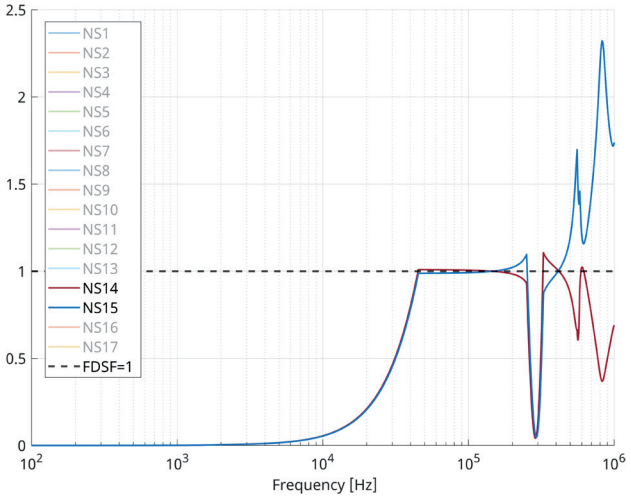

Fig. 12. FDSF of non-standard waveforms with different undershoot at the input

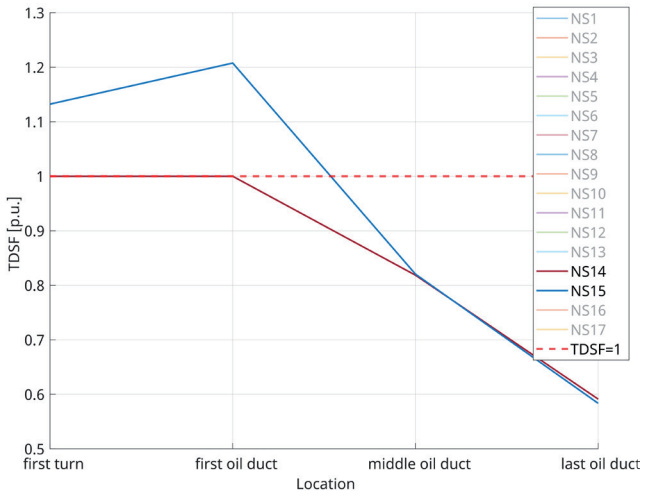

(a) Winding 5

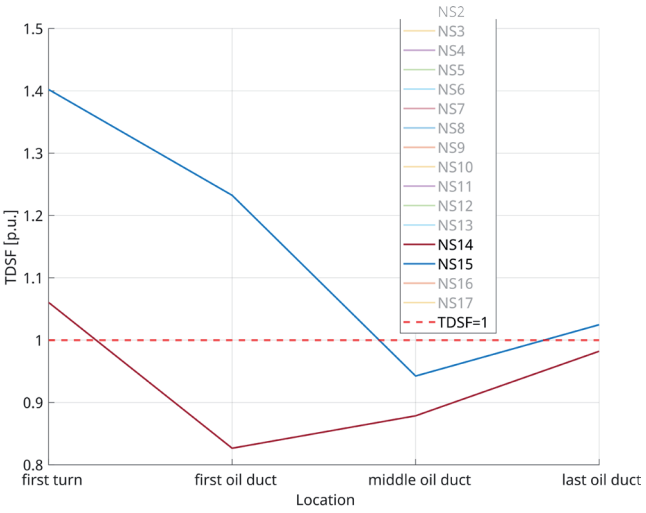

(b) Winding 1

Fig. 13. TDSF at all locations along the winding for non-standard waveforms with different undershoot

the stress decreases below unity towards the middle and end of the winding. However, for winding 1, the TDSF increases towards the end of the winding and reaches a value slightly above unity (1.02 p.u.) for the non-standard waveform with 50 % undershoot.

VI. Conclusion

This paper investigates the impact of non-standard overvoltage waveforms on different transformer disc winding types using the Frequency Domain Severity Factor (FDSF) and the Time Domain Severity Factor (TDSF). Non-standard full-wave and chopped lightning impulse waveforms were systematically derived from the standard reference impulses by varying individual waveform parameters, allowing their specific influence on winding behaviour to be isolated.

The results demonstrate that the FDSF is well suited to identifying changes in the spectral content of applied waveforms and highlighting frequency ranges in which non-standard impulses excite the transformer winding more strongly than standard test impulses. Faster front times, shorter fall times, and larger undershoots in particular introduce pronounced highfrequency components, leading to FDSF values significantly exceeding unity. However, the FDSF evaluated inside the winding generally follows the same trend as at the transformer terminals, indicating that for the investigated waveforms it provides limited insight into localized insulation stress within the winding structure.

In contrast, the TDSF proves to be more sensitive to the spatial distribution of voltage stress along the winding. While non-standard waveforms often exhibit elevated FDSF values, the corresponding TDSF results show that this does not necessarily translate into increased dielectric stress at critical insulation locations. In many cases, the maximum voltage drops across individual dielectric paths remain comparable to or lower than those caused by the standard reference impulses. Nevertheless, specific waveform characteristics, such as very fast fronts, short fall times, or high undershoot amplitudes, can lead to pronounced local stress increases at the beginning of the winding, depending on the winding design.

Overall, the study highlights that neither severity factor alone is sufficient to fully assess the insulation impact of nonstandard overvoltages. The FDSF provides valuable information on waveform severity in the frequency domain, whereas the TDSF is essential for evaluating local insulation stress within the winding. A combined application of both methods is therefore necessary for a comprehensive and physically meaningful assessment. Future work will extend the analysis to oscillatory and resonant overvoltages and further investigate the relationship between frequency-domain excitation and localized dielectric stress as well as the application of a safety margin method derived from electrical stresses.

Martin Meuser, Ebrahim Rahimpour, Morteza Eslamian, The Abilities of TDSF and FDSF in Analysing Voltage Distribution in Different Types of Disc Windings of Power Transformers, Journal of Energy, vol. 75 Number 3 (2026), 61–68
https://doi.org/10.37798/2026753781
© 2026 Copyright for this paper by authors. Use permitted under Creative Commons Attribution-NonCommercial (CC BY-NC) 4.0 International License

References

[1] International Electrotechnical Commission, *IEC 60076-3:2018 Power Transformers – Part 3: Insulation Levels, Dielectric Tests and External Clearances in Air*, Geneva, Switzerland, 2018.

[2] A. Carlson, J. Fuhr, G. Schemel, and F. Wegscheider, *Testing of Power Transformers and Shunt Reactors: Routine, Type and Special Tests*. Zurich, Switzerland: ABB AG, 2010.

[3] B. Filipovic-Gr´ ci˘ c, M. Frolov, B. Jurisic, T. Manthe, D. Matveev, and´ E. Rahimpour, "Consideration of non-standard overvoltages compared with standard overvoltages in power transformers," in *Proc. 6th International Colloquium Transformer Research and Asset Management*, Split, Croatia, Nov. 29–Dec. 2, 2023, Paper no. 144.

[4] International Electrotechnical Commission, *IEC 60071-2:2023 Insulation Co-ordination – Part 2: Application Guidelines*, Geneva, Switzerland, 2023.

[5] M. Meuser and E. Rahimpour, "Analysing of non-standard overvoltages in different types of power transformer windings using frequency domain and time domain severity factors," in *Proc. CIGRE SC A2 & D1 Joint Colloquium*, Seoul, Korea, Oct. 27–Nov. 1, 2025.

[6] W. Sima, X. Lan, Q. Yang, and T. Yuan, "Statistical analysis on measured lightning overvoltage surges in a 110 kV air-insulated substation," *IET Science, Measurement & Technology*, vol. 9, no. 1, pp. 28–36, 2015.

[7] B. Jurisic, B. Filipovic-Grcic, T. Zupan, and G. Levacic, "Statistical analysis of non-standard overvoltage waveforms measured at 220 kV terminals of a power transformer," *Electric Power Systems Research*, vol. 197, p. 107318, Aug. 2021.

[8] R. Malewski, J. Douville, and L. Lavallee, "Measurement of switching transients in 735 kV substations and assessment of their severity for transformer insulation," *IEEE Transactions on Power Delivery*, vol. 3, no. 4, pp. 1380–1390, 1988.

[9] X. M. Lopez-Fernandez, C. Alvarez-Mari´ no, et al., "Frequency domain˜ severity factor (FDSF) – Transient voltage performance – Transformer outside/inside," in *Proc. Advanced Research Workshop on Transformers*, Santiago de Compostela, Spain, Oct. 6, 2010.

[10] Joint Working Group A2/C4.39, *Electrical Transient Interaction Between Transformers and the Power System – Part I: Expertise*, Paris, France, 2014.

[11] X. M. Lopez-Fernandez and C. Alvarez-Mari´ no, "Induced transient˜ voltage performance between transformers and VCB: Severity factors and case studies," *IEEE Transactions on Power Delivery*, vol. 30, no. 3, pp. 1137–1144, 2015.

[12] C. Alvarez-Mari´ no, X. M. Lopez-Fernandez, A. J. M. J˘ a c o m o - Ramos,´ R. A. F. Castro-Lopes, and J. M. Duarte-Couto, "Time domain severity factor (TDSF): Induced transient voltage between transformer and vacuum circuit breakers," *International Journal for Computation and Mathematics in Electrical and Electronic Engineering*, vol. 31, no. 2, pp. 670–681, 2012.

https://doi.org/10.37798/2026753781

© 2026 Copyright for this paper by authors. Use permitted under Creative Commons Attribution-NonCommercial (CC BY-NC) 4.0 International License